RJC

RASĀYAN *J. Chem.*
Vol. 18 | No. 3 |1717-1724| July-September | 2025
ISSN: 0974-1496 | e-ISSN: 0976-0083 | CODEN: RJCABP
http://www.rasayanjournal.com
http://www.rasayanjournal.co.in

BIOSYNTHESIS OF SILVER NANOPARTICLES BY SOIL-DERIVED *Rhizopus arrhizus* HGS2I2: ANTIBACTERIAL POTENTIAL AGAINST CARBAPENEM-RESISTANT *Escherichia. Coli* AND *Klebsiella pneumoniae*, AND ANTIOXIDANT PROPERTIES

Himanshu Jangid[1], Anuprita Ray[1] and Gaurav Kumar[1,2,✉]
[1]School of Bioengineering and Biosciences, Lovely Professional University, Phagwara, 144411, Punjab, India
[2]Amity Institute of Microbial Technology, Amity University Rajasthan, SP-1 Kant Kalwar, NH11C, RIICO Industrial Area, 303002, Rajasthan, India
✉Corresponding author: gauravkr01@gmail.com

ABSTRACT

The increase in carbapenem-resistant *E. coli* and *Klebsiella pneumoniae* infections presents a serious public health concern due to the scarcity of effective treatment options. This study addresses this challenge by utilizing a green synthesis approach for silver nanoparticles (AgNPs) using the fungal isolate *Rhizopus arrhizus* HGS2I2. The isolate was confirmed through morphological and molecular techniques, and nanoparticle synthesis was visually verified by a change in solution color. The biogenic synthesized AgNPs are characterized using UV–Vis, dynamic light scattering (DLS), FTIR analysis, and transmission electron microscopy (TEM). The UV–Vis spectrum exhibited a peak around 420 nm, while DLS analysis showed a particle size of approximately 64.23 nm with good uniformity. TEM images revealed a spherical morphology, and FTIR spectra confirmed the presence of functional biomolecules that assist in nanoparticle stabilization. Antibacterial performance of the AgNPs was assessed through the well diffusion assay against drug-resistant isolates of *E. coli* and *K. pneumoniae*. The inhibition zones showed a clear concentration-dependent trend. *E. coli* displayed inhibition zones of 19.66 ± 0.57 mm, 17.0 ± 1.0 mm, and 14.33 ± 0.57 mm, while *K. pneumoniae* showed zones of 17.33 ± 1.52 mm, 16.33 ± 1.52 mm, and 12.33 ± 2.08 mm at concentrations of 1000, 500, and 250 µg/mL, respectively. Meropenem, used as a control, had no inhibitory effect, confirming resistance. The AgNPs showed potent antibacterial properties, with minimum inhibitory concentrations (MICs) of 10 µg/mL for carbapenem-resistant *E. coli* and 25 µg/mL for carbapenem-resistant *K. pneumoniae*. Minimum bactericidal concentrations (MBC) were determined to be 25 µg/mL and 50 µg/mL, respectively. Additionally, antioxidant activity was confirmed via DPPH assay, suggesting the biomedical relevance of the synthesized nanoparticles.

Keywords: Biogenic Silver Nanoparticles; *Rhizopus Arrhizus*; Antimicrobial Activity; Carbapenem-Resistant Bacteria; Antioxidant Potential

RASĀYAN *J. Chem.*, Vol. 18, No. 3, 2025

INTRODUCTION

Carbapenem-resistant *E. coli* and *Klebsiella pneumoniae* have become significant global health threats due to their resistance to last-line antibiotics, leading to increased mortality rates.[1] The prevalence of carbapenem resistance among Enterobacteriaceae, particularly in *E. coli* and *K. pneumoniae*, has surged in hospital settings, making treatment options highly limited. Recent studies indicate that 23.1% of *E. coli* and 52.3% of *K. pneumoniae* isolates exhibit carbapenem resistance. This resistance is mainly mediated by carbapenemase enzymes like New Delhi Metallo-β-lactamase (NDM), Oxacillinase (OXA-48)-48, and *Klebsiella pneumoniae* carbapenemase (KPC), often hosted on mobile genetic elements, enabling horizontal gene transfer.[2,3] A review of Iranian clinical isolates documented 24.0% of *K. pneumoniae* and 5.0% of *E. coli* hosting carbapenem-resistance genes, with blaOXA-48 being most prevalent. Resistance to fluoroquinolones, aminoglycosides, and polymyxins further restricts treatment.[4] As traditional antibiotics lose efficacy, alternative antimicrobial strategies are urgently required. Simultaneously, oxidative stress has been implicated in chronic diseases like cancer, neurodegeneration, and

http://doi.org/10.31788/RJC.2025.1839322

inflammation. Addressing oxidative stress through antioxidants is increasingly considered a complementary therapeutic strategy.[5] Biosynthesized silver nanoparticles (AgNPs) have demonstrated dual antimicrobial and antioxidant activity, making them promising candidates for managing infections and oxidative damage. AgNPs exhibit potent antimicrobial activity via membrane disruption, ROS generation, and DNA damage. Their synergistic activity with plant extracts, fungi, or other biomaterials enhances efficacy with reduced toxicity.[6] Fungal biosynthesis of AgNPs is a promising alternative to chemical synthesis due to its eco-friendliness, biocompatibility, and stability. *Rhizopus arrhizus* is recognized for its extracellular enzymes capable of reducing silver ions into nanoparticles. These AgNPs typically exhibit controlled morphology and size (10–100 nm), enhancing biological activity.[7] Biosynthesized AgNPs from fungi and medicinal plants have shown effectiveness against MDR pathogens, including CREC and CRKP. Their mechanisms involve membrane penetration, oxidative stress induction, and DNA disruption. Studies report inhibition zones of 10–19 mm for *E. coli* and *K. pneumoniae*, surpassing traditional antibiotics. Additionally, AgNPs exhibit significant antioxidant activity, such as free radical scavenging and enhancement of antioxidant enzymes.[8] For instance, AgNPs synthesized from *Cinnamomum verum* demonstrated 92% radical scavenging efficiency.[9] This study aims to explore the biosynthesis, antibacterial, and antioxidant potential of AgNPs synthesized using soil-derived *Rhizopus arrhizus* HGS2I2, contributing to sustainable nanotechnology-based approaches against drug-resistant pathogens and oxidative stress-related diseases.

EXPERIMENTAL

Sample Collection

Soil samples were gathered from a depth of 5–10 cm beneath decomposing organic matter in Phagwara, Punjab, India (Latitude: 31.22° N, Longitude: 75.77° E). Using sterile spatulas, the soil was collected and transferred into sterile, airtight containers. All samples were handled under sterile conditions and immediately transported to the laboratory. Upon arrival, they were stored at 4 °C until further processing for fungal isolation.[10]

Isolation of a Fungal Isolate

The fungal strains were isolated by performing serial dilutions followed by spread plating on potato dextrose agar (PDA). A 1-gram soil sample was subjected to a dilution series ranging from 10^{-1} to 10^{-5} using sterile distilled water. Measured volumes from each dilution were plated on PDA and were maintained at 28 °C for 3–5 days. Subsequent identification of fungal isolates was based on cultural traits, morphological features, and ITS sequencing.[10]

Identification of Fungal Isolate

Fungal colonies showing characteristic white, cottony mycelium that later turned grayish-black were selected and subcultured to obtain pure cultures. Morphological identification was carried out using lactophenol cotton blue staining and examined under a light microscope, observing key features such as rhizoids, sporangiophores, and sporangia. Molecular identification was done by extracting the genomic DNA from the cultures, and the ITS regions were amplified using the ITS1 and ITS4 primers employing the PCR method. The PCR reaction mixture included genomic DNA, primers, dNTPs, buffer, $MgCl_2$, and Taq DNA polymerase in appropriate concentrations. The amplified product was sequenced by Sanger sequencing and identified with the help of BLASTn in the NCBI GenBank and deposited in GenBank.[11]

Fungal Extract Preparation

The fungal strain was initially grown on PDA and incubated at 28 °C for 3 days to encourage mycelial development. Later, 100 mL of sterilized potato dextrose broth (PDB) was inoculated with 1 mL of fungal spore suspension. This culture was incubated under static conditions at 28 °C for 5 days. Post incubation, the fungal biomass was cleaned by discarding the liquid medium and thoroughly rinsed with autoclaved distilled water to remove any remaining media. The biomass was then resuspended in 100 mL of sterile water and agitated at 100–120 rpm for 1–2 days to aid in the release of intracellular metabolites. The resulting liquid was collected and used as the fungal extract for silver nanoparticle synthesis.[12]

Biosynthesis of Silver Nanoparticles

To carry out nanoparticle synthesis, 1 mL of the fungal extract was added to 19 mL of 1 mM $AgNO_3$ solution under sterile conditions. For control, 1 mL of the same extract was mixed with 19 mL of distilled water. Both mixtures were kept under controlled lab conditions. The formation of AgNPs was visually confirmed through a noticeable color change and further validated via UV–Visible spectroscopy.[12]

Characterization of Biogenically Synthesized Silver Nanoparticles

The biogenic synthesized AgNPs were characterized using multiple analytical methods such as UV–Vis, FTIR, DLS, and TEM. UV–Vis spectroscopy was used to track nanoparticle formation by detecting surface plasmon resonance in the range of 200–800 nm. FTIR analysis provided insights into the functional groups responsible for reducing and stabilizing the nanoparticles, based on spectral data ranging from 4000 to 400 cm^{-1}. DLS was utilized to evaluate particle size distribution and zeta potential, offering information about colloidal stability. TEM offered visual confirmation of the shape and structural features of the nanoparticles.[13]

Antimicrobial Activity

The bactericidal effectiveness of the biogenic synthesized AgNPs was tested against carbapenem-resistant strains of *K. pneumoniae* and *E. coli*, collected from the Punjab Institute of Medical Sciences (PIMS), Jalandhar. Antimicrobial assessment was carried out using the agar well diffusion assay. Mueller–Hinton Agar (MHA) plates were inoculated with bacterial cultures adjusted to a 0.5 McFarland standard. Using a sterile cork borer, 9 mm wells were punched into the agar medium. Each well received 100 µL of AgNP solution at varying concentrations—1000, 500, and 250 µg/mL—prepared in sterile distilled water. Meropenem disk (10 µg/mL) served as a positive control, and autoclaved double-distilled water served as a negative control. The plates were incubated at 37 °C for 18 to 24 hours. Post incubation, the antibacterial effect was assessed by measuring the diameters of the inhibition zones formed around each well.[14]

MIC and MBC

The MIC of the biosynthesized silver nanoparticles was tested using the broth microdilution technique. AgNP stock solutions ranging from 5 to 200 µg/mL were prepared in MHB. Since the bacterial inoculum was added later, each nanoparticle solution was prepared at twice the intended final concentration (i.e., 10–400 µg/mL). In a sterile 96-well microplate, 100 µL of each nanoparticle dilution was added, followed by 100 µL of bacterial culture adjusted to a 0.5 McFarland standard (approximately 1.5×10^8 CFU/mL). The plates were incubated at 37 °C for 20–24 hours. MIC was noted as the lowest nanoparticle concentration at which no visible turbidity occurred, indicating inhibition of bacterial growth.[15] For determining the minimum bactericidal concentration (MBC), 10 µL from wells that showed no visible bacterial growth were transferred onto fresh MHA plates. These plates were incubated for 24 hours at 37 °C. The MBC was recorded as the minimum concentration of nanoparticles that completely eliminated bacterial colonies. All experiments were performed in triplicate to ensure accuracy and reproducibility.[15]

Antioxidant Activity

Biogenically synthesized AgNPs' antioxidant potential was tested using the DPPH assay. Nanoparticle extracts were tested at varying concentration ranges from 10 to 100 µg/mL. For each concentration, 2 mL of a DPPH solution (0.2 mM) was added to the sample and mixed well, and then further incubated in the dark at 37 °C for 30 minutes to minimize degradation caused by light exposure. Absorbance readings were taken at 517 nm using a UV–Vis spectrophotometer, where methanol served as the reference blank. Ascorbic acid served as a standard antioxidant. The scavenging efficiency was determined using the appropriate formula for DPPH radical inhibition.[16]

$$\% \text{ DPPH radical scavenging} = [(A_c - A_t)/Ac] \times 100$$

Here, A_c Absorbance control (DPPH), A_t Absorbance sample.

Statistical Analysis

All experimental procedures were carried out in three independent replicates. Results are presented as average values along with their corresponding standard deviations (± SD). Data processing and statistical evaluations were performed using GraphPad Prism software.

RESULTS AND DISCUSSION

This study successfully showed the green synthesis of AgNPs utilizing *Rhizopus arrhizus* HGS2I2. The biosynthesized AgNPs exhibited significant antimicrobial and antioxidant properties. The findings confirm the effectiveness of these biogenic nanoparticles in inhibiting carbapenem-resistant *E. coli* and *K. pneumoniae*, which are among the most clinically concerning multidrug-resistant pathogens.

Isolation and Molecular Characterization of Fungal Isolate

The fungal strain used in this study was isolated from soil collected in Phagwara, Punjab, India. Initial fungal growth appeared after incubating soil suspensions on PDA plates for 3 days at 28 °C. The strain was further purified by repeated subculturing, which resulted in the development of a cottony white mycelium that later turned grayish-black in appearance (Fig. 1A, B). For morphological assessment, lactophenol cotton blue staining was performed to examine structural features such as sporangia, sporangiospores, rhizoids, and sporangiophores, which are characteristic of the *Rhizopus* genus (Fig. 1C). For molecular confirmation, genomic DNA was isolated, and the ITS region amplified using ITS4 and ITS1 primers through polymerase chain reaction (PCR). The resulting sequences were analyzed using the BLAST tool and submitted to the NCBI GenBank (Accession No: PV361847.1), confirming the identity as *Rhizopus arrhizus* HGS2I2. The phylogenetic analysis is depicted in Fig. 1D.

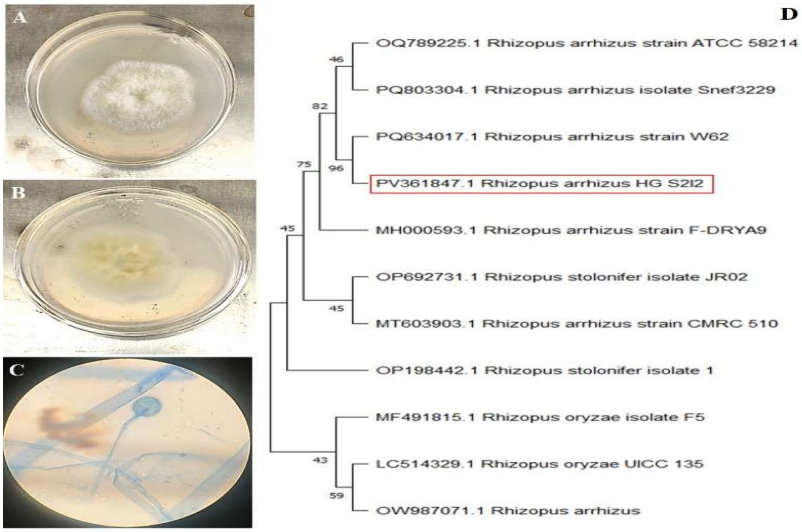

Fig.-1: Isolation and Characterization of Fungal Isolate Here (A) Colonial Morphology on PDA Plate Front Side Image, (B) Back Side Image, And (C) Phylogenetic Tree

Characterization of Biogenic Silver Nanoparticles

The formation of AgNPs was verified through a visible color transformation, which indicated the reduction in silver ions by metabolites present in the intracellular fungal extract. For synthesis, a reaction mixture comprising 1 mL of the fungal extract and 19 mL of 1 mM $AgNO_3$ was prepared. Control samples lacked $AgNO_3$ and included only sterile distilled water and fungal extract. After 48 hours of incubation, the appearance of a brown color confirmed nanoparticle formation (Fig. 2A). The lack of color change in the control group further supported the role of the fungal extract in reducing Ag^+ ions. The confirmation of nanoparticle synthesis and analysis of their optical properties was carried out using UV-Visible spectroscopy. The UV-Vis spectra displayed a SPR peak at 420 nm, which shows AgNPs formation and supports successful silver ion reduction. These spectral observations were consistent with previously reported features of biogenically synthesized AgNPs.[17] Particle size analysis was done using DLS. The hydrodynamic diameter of the synthesized AgNPs was found to be approximately 64.23 nm,

indicating their nanoscale size. The sharp peak distribution indicated that the nanoparticles were uniform in size and exhibited stable dispersion, making them suitable for biological applications (Fig. 2 B). These findings align with previous reports on DLS-based AgNP characterization.[20]

FTIR was used to check the functional groups involved in the bioreduction and stabilization of the biogenic synthesized AgNPs. The FTIR spectra revealed distinct absorption bands at 3225, 1614, 1290, 1118, and 774 cm^{-1}. These signals correspond to stretching vibrations associated with hydroxyl (O-H), amine (N-H), carbonyl (C=O), and amide (C-N) functional groups. The peaks indicate that proteins, polysaccharides, and other biomolecules present in the fungal extract contributed to nanoparticle formation by acting as reducing and capping agents (Fig.-2C). This capping prevents nanoparticle aggregation and improves colloidal stability. Similar functional groups have been reported in earlier green synthesis studies, where O-H and N-H stretching were linked to phenolic and amine-containing compounds that aid in nanoparticle stabilization. These biomolecules not only help in silver ion reduction but also offer a protective coating that maintains particle dispersion. The obtained spectral data support the involvement of these biomolecules and suggest a biosynthesis mechanism consistent with previous literature.[18,19] TEM analyzed the size, shape, and dispersion of the biosynthesized AgNPs. The TEM image reveals well-dispersed nanoparticles with a uniform shape and size distribution. The nanoparticles appear mostly spherical to slightly irregular, with an average size of 64.23 nm (Fig.-2D, E). The clear visibility and distribution of nanoparticles suggest minimal aggregation, confirming their stability. For instance, biosynthesized AgNPs using *Hyssopus officinalis* extract were shown to form stable, monodisperse spherical particles ranging from 16–36 nm, with size and dispersion strongly influenced by the plant's phytochemicals acting as capping and stabilizing agents. Similarly, *Crataegus gracilior* leaf extract produced predominantly spherical AgNPs (20–50 nm), confirmed by TEM, with FTIR supporting the role of bioactive compounds in surface capping.[21]

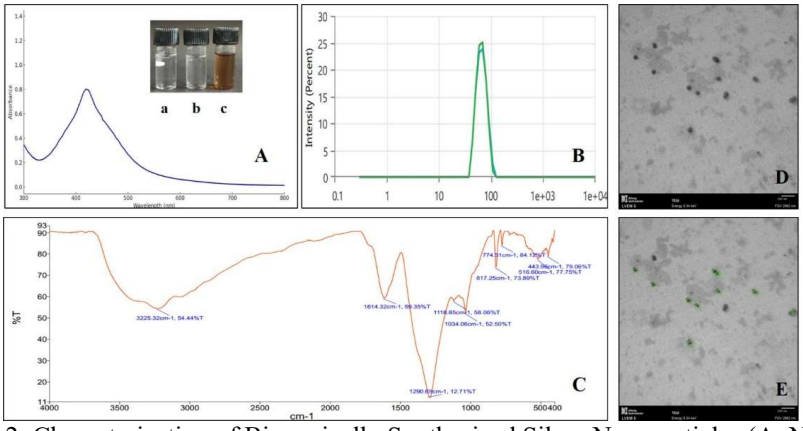

Fig.-2: Characterization of Biogenically Synthesized Silver Nanoparticles (AgNPs).
Here (A) UV-Vis Spectrum; Inset: (a) $AgNO_3$ Solution (1mM), (b) Intracellular Fungal Extract, (c) Formation of AgNPs Indicated by a Color Change, (B) DLS Analysis, (C) FTIR Spectrum, and (D & E) TEM Analysis

Biological Properties of Biogenic Silver Nanoparticles

The antibacterial potential of AgNPs synthesized via fungal extracts was tested using the agar well diffusion method against carbapenem-resistant *E. coli* and *K. pneumoniae* (Table 1). The nanoparticles were tested at concentrations of 1000, 500, and 250 µg/mL. Negative control set using autoclaved distilled water, while Meropenem (10 µg/mL) served as the positive control. The results demonstrated a concentration-dependent inhibition pattern. For *E. coli*, the mean zone of inhibition values were 19.66 ± 0.57 mm, 17.00 ± 1.00 mm (Fig.-3A), and 14.33 ± 0.57 mm at 1000, 500, and 250 µg/mL (Fig.-3B), respectively. In the case of *K. pneumoniae*, the inhibition zones measured 17.33 ± 1.52 mm, 16.33 ± 1.52 mm, and 12.33 ± 2.08 mm, respectively. No antibacterial activity was observed in the negative control group, and Meropenem failed to inhibit either strain, highlighting their carbapenem resistance. In contrast, AgNPs exhibited substantial antibacterial properties, emphasizing their potential as an alternative therapeutic approach. These results reinforce the application of AgNPs as a promising

strategy against multidrug-resistant bacteria, particularly due to their unique, non-enzymatic mode of action that lowers the chance of resistance development.

The MIC of the AgNPs was found using broth dilution assays to assess the lowest concentration capable of inhibiting visible bacterial growth. For *Escherichia coli*, the MIC was found to be 10 µg/mL, indicating a strong inhibitory effect at a relatively low concentration. In contrast, *Klebsiella pneumoniae* exhibited a higher MIC value of 25 µg/mL, suggesting a moderately reduced sensitivity to AgNPs.

Table 1: Zone of Inhibition (mm ± SD) n=3 of biosynthesized AgNPs against Carbapenem-Resistant *E. coli* and *K. pneumoniae*

Bacterial Strain	AgNPs Concentration			Negative control (Distilled Water)	Positive control (Meropenem at 10µg/ml)
	1000 µg/mL	500 µg/mL	250 µg/mL		
Carbapenem-resistant *E. coli*	19.66±0.57	17.0 ± 1.0	14.33±0.57	0 ± 0	0 ± 0
Carbapenem-resistant *K. pneumoniae*	17.33±1.52	16.33±1.52	12.33±2.08	0 ± 0	0 ± 0

These results highlight the effective bacteriostatic activity of AgNPs, particularly against carbapenem-resistant *E. coli*. The MBC was evaluated to determine the lowest concentration of AgNPs required to achieve bacterial killing rather than just inhibition. For *E. coli*, the MBC was established at 25 µg/mL, whereas *K. pneumoniae* required a higher concentration of 50 µg/mL to achieve a complete bactericidal effect. The increase in concentration from MIC to MBC for both strains demonstrates that while AgNPs exhibit potent inhibitory effects, higher doses are required for full eradication. This distinction between MIC and MBC confirms the dual action of AgNPs as both bacteriostatic and bactericidal agents, depending on the concentration applied. This finding aligns with previous observations regarding MIC and MBC of silver nanoparticles against multidrug-resistant bacteria. The antioxidant potential of biogenic AgNPs was tested using the DPPH assay (C). A significant ($p < 0.001$) dose-dependent increase in DPPH radical scavenging activity was seen, with an IC50 value of 118.83µg/mL indicating strong antioxidant activity. This finding aligns with previous observations regarding the free radical neutralizing capacity of biosynthesized AgNPs and supports their potential in mitigating oxidative stress.[22]

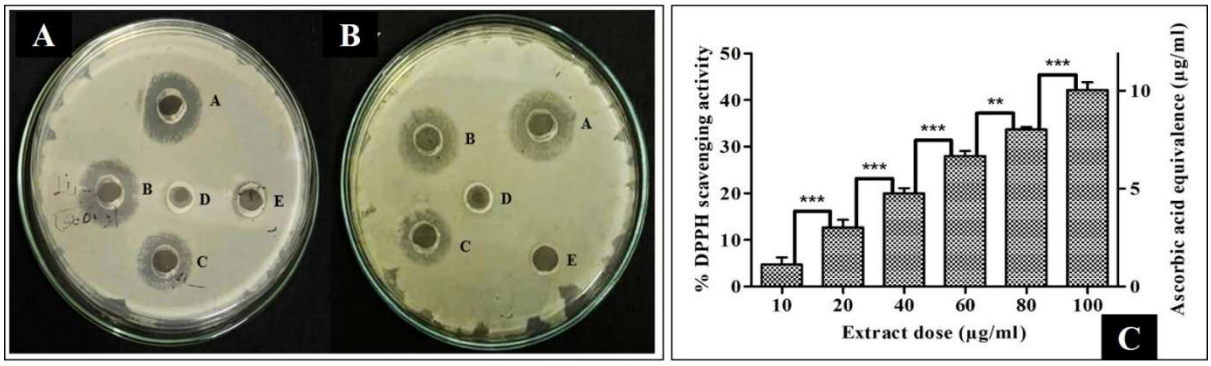

Fig.-3: Pharmacological Properties of Biogenically Synthesized Silver Nanoparticles. Here (A & B) Antimicrobial Activity Against Carbapenem-Resistant (A) *E. Coli* (B) *K. Pneumoniae*, Using the Agar Well Diffusion Method and (C) DPPH Assay of Biogenic AgNPs

CONCLUSION

This study showed the biosynthesis of AgNPs from *Rhizopus arrhizus* HGS2I2 and established their antimicrobial, antioxidant, and structural properties. Characterization methods (UV-Vis, FTIR, DLS, TEM) confirmed the synthesis of well-dispersed, biomolecule-stabilized AgNPs with a mean diameter of ~64 nm. The AgNPs were highly effective against carbapenem-resistant *K. pneumoniae* and *E. coli*, effectively inhibiting bacterial growth when conventional antibiotics (Meropenem) were unsuccessful. The MIC and MBC values were found to be 10 µg/mL and 25 µg/mL for *E. coli*, and 25 µg/mL and 50 µg/mL for *K. pneumoniae*, confirming their strong bacteriostatic and bactericidal effects. Additionally, the AgNPs exhibited notable antioxidant potential, reinforcing their biomedical applicability. These

findings highlight the promising role of biosynthesized AgNPs as an alternative antimicrobial strategy, particularly against multidrug-resistant pathogens. Given their potent antibacterial efficacy and broad bioactivity, further studies should focus on mechanistic insights, in vivo applications, and toxicity evaluations to advance their clinical potential and ensure safe therapeutic use. This work aligns with SDG-3: Good Health and Well-being, by contributing to the development of alternative antimicrobial strategies against resistant pathogens.

ACKNOWLEDGMENTS

The authors acknowledge and extend their appreciation to the Genexplore Diagnostics and Research Centre Pvt. Ltd. for gene sequencing and the Punjab Institute of Medical Sciences (PIMS), Jalandhar, for providing cultures. The authors also like to thank Lovely Professional University and Amity University, Rajasthan, for providing the necessary facilities for the conduct of this research.

CONFLICT OF INTERESTS

The authors declare that there is no conflict of interest.

AUTHOR CONTRIBUTIONS

The present work is related to *SDG-3: Good Health and Well-being*. All the authors contributed significantly to this manuscript, participated in reviewing/editing, and approved the final draft for publication. The research profile of the authors can be verified from their ORCID ids, given below:

Himanshu Jangid https://orcid.org/0009-0005-9919-5905
Anuprita Ray https://orcid.org/0000-0002-0352-4024
Gaurav Kumar https://orcid.org/0000-0002-9464-7811

REFERENCES

1. T. Karampatakis, K. Tsergouli and P. Behzadi, *Antibiotics*, **12**, 234(2023), https://doi.org/10.3390/antibiotics12020234
2. K. Arumugam, G. S. Karande and S. R. Patil, *Cureus*, **16**, e70918, https://doi.org/10.7759/cureus.70918
3. T. Tesfa, H. Mitiku, M. Edae and N. Assefa, *Systematic Reviews*, **11**, 240(2022), https://doi.org/10.1186/s13643-022-02110-3
4. R. Ghotaslou, B. Salahi, G. Naderi and N. Alizadeh, *Infection & Chemotherapy*, **55**, 90(2023), https://doi.org/10.3947/ic.2022.0160
5. Á. Mourenza, J. A. Gil, L. M. Mateos and M. Letek, *Antioxidants*, **9**, 361(2020), https://doi.org/10.3390/antiox9050361
6. P. R. More, S. Pandit, A. D. Filippis, G. Franci, I. Mijakovic and M. Galdiero, *Microorganisms*, **11**, 369(2023), https://doi.org/10.3390/microorganisms11020369
7. M. Guilger-Casagrande and R. de Lima, *Frontiers in Bioengineering and Biotechnology*, **7**, 287(2019), https://doi.org/10.3389/fbioe.2019.00287
8. M. Tariq, K. N. Mohammad, B. Ahmed, M. A. Siddiqui and J. Lee, *Molecules*, **27**, 4754(2022), https://doi.org/10.3390/molecules27154754
9. A. Mohamed, M. Dayo, S. Alahmadi and S. Ali, *Nanomaterials*, **14**, 1383(2024), https://doi.org/10.3390/nano14171383
10. R. Thakor, H. Mistry, H. Patel, D. Jhala, N. Parmar and H. Bariya, *Journal of Applied Microbiology*, **133**, 857(2022), https://doi.org/10.1111/jam.15611
11. L. Zakaria, M. I. M. Jamil and I. S. M. Anuar, *Tropical Life Sciences Research*, **27**, 153(2016).
12. A. M. Othman, M. A. Elsayed, N. G. Al-Balakocy, M. M. Hassan and A. M. Elshafei, *Journal of Genetic Engineering and Biotechnology*, **17**, 8(2019), https://doi.org/10.1186/s43141-019-0008-1
13. S. Raj, R. Trivedi and V. Soni, *Surfaces*, **5**, 1(2022), https://doi.org/10.3390/surfaces5010003

14. R. M. Humphries et al., *Journal of Clinical Microbiology*, **56**, e01934-17(2018), https://doi.org/10.1128/JCM.01934-17
15. S. Gurunathan, *Arabian Journal of Chemistry*, **12**, 168(2019), https://doi.org/10.1016/j.arabjc.2014.11.014
16. S. Baliyan et al., *Molecules*, **27**, 1326(2022), https://doi.org/10.3390/molecules27041326
17. J. Ferdous et al., *The Microbe*, **4**, 100111(2024), https://doi.org/10.1016/j.microb.2024.100111
18. J. Das and P. Velusamy, *Materials Research Bulletin*, **48**, 4531(2013), https://doi.org/10.1016/J.MATERRESBULL.2013.07.049
19. A. Zuhrotun, D. J. Oktaviani and A. N. Hasanah, *Molecules*, **28**, 3240(2023), https://doi.org/10.3390/molecules28073240
20. A. Almatroudi, *Open Life Sciences*, **15**, 819(2020), https://doi.org/10.1515/biol-2020-0094
21. A. Balciunaitiene et al., *Molecules*, **27**, (2022), https://doi.org/10.3390/molecules27227700
22. P. Moteriya and S. Chanda, *Journal of Genetic Engineering and Biotechnology*, **16**, 105(2018), https://doi.org/10.1016/j.jgeb.2017.12.003

[RJC-9322/2025]